

## Evaluation of scale invariance in physiological signals by means of balanced estimation of diffusion entropy

Wenqing Zhang,<sup>1</sup> Lu Qiu,<sup>1</sup> Qin Xiao,<sup>1</sup> Huijie Yang,<sup>1,\*</sup> Qingjun Zhang,<sup>2</sup> and Jianyong Wang<sup>3</sup>

<sup>1</sup>*Business School, University of Shanghai for Science and Technology, Shanghai 200093, China*

<sup>2</sup>*Analysis and Testing Center, Hebei United University, Tangshan 063009, Hebei Province, China*

<sup>3</sup>*Department of Physics, Xingtai College, Xingtai 054001, Hebei Province, China*

(Received 4 May 2012; revised manuscript received 14 September 2012; published 12 November 2012)

By means of the concept of the balanced estimation of diffusion entropy, we evaluate the reliable scale invariance embedded in different sleep stages and stride records. Segments corresponding to waking, light sleep, rapid eye movement (REM) sleep, and deep sleep stages are extracted from long-term electroencephalogram signals. For each stage the scaling exponent value is distributed over a considerably wide range, which tell us that the scaling behavior is subject and sleep cycle dependent. The average of the scaling exponent values for waking segments is almost the same as that for REM segments ( $\sim 0.8$ ). The waking and REM stages have a significantly higher value of the average scaling exponent than that for light sleep stages ( $\sim 0.7$ ). For the stride series, the original diffusion entropy (DE) and the balanced estimation of diffusion entropy (BEDE) give almost the same results for detrended series. The evolutions of local scaling invariance show that the physiological states change abruptly, although in the experiments great efforts have been made to keep conditions unchanged. The global behavior of a single physiological signal may lose rich information on physiological states. Methodologically, the BEDE can evaluate with considerable precision the scale invariance in very short time series ( $\sim 10^2$ ), while the original DE method sometimes may underestimate scale-invariance exponents or even fail in detecting scale-invariant behavior. The BEDE method is sensitive to trends in time series. The existence of trends may lead to an unreasonably high value of the scaling exponent and consequent mistaken conclusions.

DOI: [10.1103/PhysRevE.86.056107](https://doi.org/10.1103/PhysRevE.86.056107)

PACS number(s): 89.75.Fb, 05.45.-a, 05.40.-a

### I. INTRODUCTION

Scale invariance embedded in physiological signals can shed light on mechanisms of dynamical processes occurring in the human body, based upon which one can construct theoretical models of the processes and evaluate the state of health of disease sufferers [1,2]. A typical example is the scaling behavior in different sleep stages. A cycle of healthy sleep persists typically for 1 to 2 h, which constitutes a sequence of sleep stages including waking, light sleep, rapid eye movement (REM) sleep, and deep sleep. Little is known about the specific functions of these circadian rhythms. It is believed that the deep and REM sleep states are essential for physical recreation and memory reconsolidation, respectively. Extensive work has shown that heartbeat dynamics is characterized by long-range correlations, and different long-range exponents are found for healthy people and patients suffering from disease [3], and for different sleep stages [4]. In particular, among the different sleep stages, long-range correlation occurs solely during REM sleep, which is similar to, while less pronounced than, that during wakefulness. Hence, scale invariance embedded in heartbeat intervals can be used as a monitor of intrinsic neural-autonomic regulation of the circadian rhythms, which may find a potential use in disease diagnosis and therapy. But evaluation of scale invariance in physiological signals meets two challenges.

Methodologically, variance-based methods, such as wavelet analysis [5] and the detrended fluctuation approach [6], are widely reported in the literature for calculation of scaling

exponents. They can estimate correctly the values of the scaling exponents for fractional Brownian motion, but incorrectly those for Levy walks, and cannot even find the scaling-invariant behavior existing in a Levy flight process due to divergency of the second moment [7]. A successful complementary method is diffusion entropy analysis. From a stationary time series, one can construct all possible segments with a specified length. Regarding the length as the time duration, each segment can be regarded as a trajectory of a particle starting from the original point. The time series is then mapped to an ensemble with the trajectories being realizations of a stochastic motion. From the distribution function of the displacement one can calculate the Shannon entropy, which is called the diffusion entropy by Scafetta *et al.* [7]. Detailed work has proved its power in evaluation of scaling exponents for both fractional Brownian and Levy motions [8].

In practice, to obtain the probability distribution function, we divide the region of distribution of the displacement into many bins and reckon the number of displacements occurring in each bin. The probability occurring at a bin is generally approximated by the relative frequency, namely, the ratio between the number occurring and the total number of realizations, which is perfect for an ensemble with an infinite number of realizations. However, a physiological signal is generally very short. Sometimes we can obtain a long time series, but some phase transitions occur in the measurement duration, which separate the series into short segments with different scaling behaviors. For example, a typical cycle of healthy sleep contains several thousands of heartbeat intervals, in which a sequence of transitions occurs between different sleep stages. Figure 2(a) presents a long-term heartbeat interval

\*Corresponding author: [hjyang@ustc.edu.cn](mailto:hjyang@ustc.edu.cn)

series for a healthy subject. The lengths for waking, REM sleep, light sleep, and deep sleep stages are distributed in wide regions from  $10^1$  to  $10^3$  without characteristic lengths (see Sec. II C).

A short length of a time series may induce large statistical fluctuations and/or bias in physical quantities such as probability, moment, and entropy [9]. In a recent paper, Bonachela *et al.* [10] reviewed the attempts at devising improved estimators of entropy for small data sets and propose accordingly a balanced estimator that performs well when the data sets are small. In one of our recent papers, we proposed a concept called the balanced estimator of diffusion entropy (BEDE) [11], in which the original form of the entropy in diffusion entropy analysis is replaced by a balanced estimator of entropy. Calculations show that it gives reliable scaling exponents for short time series with length  $\sim 10^2$ .

In the present paper, the BEDE method is used to evaluate scaling behaviors in heartbeat series for different sleep stages and stride time series for normal, fast, and slow walkers. Results show that for finite records of physiological signals the current methods in the literature may lead to unacceptable errors for scaling exponents and wrong conclusions, while the BEDE approach can provide us with a reliable estimation of scaling exponents.

## II. METHOD AND MATERIALS

### A. Diffusion entropy

Let us review briefly the concept of diffusion entropy [7] proposed to detect scale invariance in stationary series. For a stationary time series  $\xi_1, \xi_2, \dots, \xi_N$ , all the possible segments with specified length  $s$  read

$$X_i(s) = \{\xi_i, \xi_{i+1}, \dots, \xi_{i+s-1}\}, \quad i = 1, 2, \dots, N - s + 1. \quad (1)$$

We regard the length  $s$  as time and consequently  $X_i(s)$  is the  $i$ th realization of a stochastic process. The total  $N - s + 1$  realizations form an ensemble of the process. The displacement of the  $i$ th realization reads

$$x_i(s) = \sum_{j=i}^{i+s-1} \xi_j. \quad (2)$$

Dividing the interval in which the displacements occur into  $M(s)$  bins, one can reckon the number of displacements occurring in each bin, denoted by  $n(k, s)$ ,  $k = 1, 2, \dots, M(s)$ . The probability distribution function can be approximated by the relative frequency

$$p(k, s) \sim \hat{p}(k, s) = \frac{n(k, s)}{N - s + 1}, \quad k = 1, 2, \dots, M(s). \quad (3)$$

The consequent naive approximation of the Shannon entropy reads

$$S_{DE}(s) \sim S_{DE}^{\text{naive}}(s) = - \sum_{k=1}^{M(s)} \hat{p}(k, s) \ln[\hat{p}(k, s)]. \quad (4)$$

Provided the stochastic process behaves in a scale-invariant way, we have

$$p(k, s) \sim \frac{1}{s^\delta} F\left(\frac{x_{\min}(s) + (k - 0.5)\epsilon(s)}{s^\delta}\right), \quad (5)$$

$$k = 1, 2, \dots, M(s),$$

where  $\epsilon(s)$  is the size of the bin, which is simply selected to be a certain fraction of the standard deviation of the initial series. Plugging Eq. (5) into Eq. (4) leads to

$$S_{DE}(s) = - \int_{-\infty}^{+\infty} dy F(y) \ln[F(y)] + \delta \ln(s) = A + \delta \ln(s). \quad (6)$$

The diffusion entropy (DE) has been used as a powerful method to evaluate scaling invariance embedded in time series in diverse fields, such as solar activity [12], spectra of complex networks [13], physiological signals [14], DNA sequences [15], geographical phenomena [16], and finance [17].

### B. Balanced estimation of diffusion entropy

Unfortunately, extension of Eq. (6) to the naive approximation of diffusion entropy is a nontrivial step, i.e., generally  $S_{DE}^{\text{naive}}(s) \neq A + \delta \ln(s)$  [9]. Defining the relative error as  $\mu(k, s) \equiv \frac{\hat{p}(k, s) - p(k, s)}{p(k, s)}$ , after a straightforward computation we have

$$S_{DE}(s) = S_{DE}^{\text{naive}} + \frac{M(s) - 1}{2(N - s + 1)} + O(M(s)). \quad (7)$$

The leading order of error,  $\frac{M(s)-1}{N-s+1}$ , vanishes as  $N - s \rightarrow \infty$ , while it may become unacceptably large when  $N - s$  is finite. Especially for short time series the linear relation in Eq. (6) will be distorted completely and one cannot find scaling-invariant behavior. In the naive approximation of diffusion entropy there exist simultaneously statistical error (variance) and systematic error (bias). That is,  $\hat{p}(k, s) \ln[\hat{p}(k, s)]$  is not an acceptable estimation of its corresponding term  $p(k, s) \ln[p(k, s)]$ . Hence, our task is to find a different estimation of  $p(k, s) \ln[p(k, s)]$ , denoted by  $\hat{S}_{DE}[n(k, s)]$ , which minimizes the combination of variance and bias. Here, we ignore correlations between  $n(k, s)$ ,  $k = 1, 2, \dots, M(s)$ .

We employ the solution proposed by Bonachela *et al.* [10]. Mathematically, this problem can be formulated as

$$\frac{\partial \Delta^2(k, s)}{\partial \hat{S}_{DE}[n(k, s)]} = 0,$$

$$\Delta^2(k, s) = \int_0^1 [\Delta_{\text{bias}}^2(k, s) + \Delta_{\text{stat}}^2(k, s)] \times w[p(k, s)] dp(k, s), \quad (8)$$

where

$$\Delta_{\text{bias}}^2(k, s) = (p(k, s) \ln[p(k, s)] - \langle \hat{S}_{DE}[n(k, s)] \rangle)^2,$$

$$\Delta_{\text{stat}}^2(k, s) = (\langle \hat{S}_{DE}[n(k, s)] \rangle - \langle \hat{S}_{DE}[n(k, s)] \rangle)^2 \quad (9)$$

are the bias and variance, respectively, and  $w[p(k, s)]$  is a weight function depending on the specific problem. Generally, we set  $w[p(k, s)] = 1$  due to lack of extra knowledge. The average  $\langle \cdot \rangle$  is obtained by using the binomial distribution

function

$$P_{n(j,s)}[p(j,s)] = \frac{[N-s+1]!}{n(j,s)![N-s+1-n(j,s)]!} \times [p(j,s)]^{n(j,s)} [1-p(j,s)]^{N-s+1-n(j,s)}. \quad (10)$$

A simple computation leads to Ref. [11]

$$\hat{S}_{DE}[n(k,s)] = \frac{n(j,s)+1}{N-s+3} \sum_{k=n(j,s)+2}^{N-s+3} \frac{1}{k}. \quad (11)$$

Consequently, a proper estimation of  $S_{DE}(s)$  reads

$$\hat{S}_{DE}(s) = \frac{1}{N-s+3} \sum_{j=1}^{M(s)} [n(j,s)+1] \sum_{k=n(j,s)+2}^{N-s+3} \frac{1}{k}, \quad (12)$$

which is called the balanced estimator of diffusion entropy.

### C. Materials

We consider long-term electroencephalogram (EEG) signals for a total of 16 male subjects aged from 32 to 56 (mean age 43), with weights from 89 to 152 kg (mean weight 119 kg) [18]. Each EEG record persists on average for 7.5 h annotated with sleep staging and apnea information. Each annotation applies to the 30 s following it. Sleep stages are divided into four stages, namely, deep sleep, light sleep, REM sleep, and waking phase, which are determined by using visual evaluation of electrophysiological recordings of brain activity.

We consider also the stride series for a total of ten young healthy volunteers, denoted by si01, si02, ..., si10 [19]. "Healthy" here indicates that the participants have no history of any neuromuscular, respiratory, or cardiovascular disorders and are taking no medication. The age distribution is 18 to 29 yr. The average age is 21.7 yr. The height and weight are centered at 177 cm and 71.8 kg, with standard deviations of 8 cm and 10.7 kg, respectively. All the subjects walk continuously on level ground around an obstacle-free, long (either 225 or 400 m), approximately oval path. The stride interval is measured by using an ultrathin, force-sensitive switch taped inside one shoe. Each subject walks for four trials, including slow, normal, fast, and metronome-regulated. For the slow, normal, and fast trials the mean stride intervals are  $1.3 \pm 0.2$ ,  $1.1 \pm 0.1$ , and  $1.0 \pm 0.1$  m, and the mean walking rates are  $1.0 \pm 0.2$ ,  $1.4 \pm 0.1$ , and  $1.7 \pm 0.1$  m/s, respectively.

The scale invariance embedded in heartbeat and stride interval series, denoted by  $\{y_1^O, y_2^O, \dots, y_N^O\}$ , is evaluated. The key step in using the BEDE method is to guarantee the considered series being stationary [20]. The centered moving average method [21] is employed to obtain the trend of a time series; namely, from the original series we calculate its trend  $y^T$ , where the elements read

$$y_i^T = \frac{1}{s} \sum_{j=-[(s+1)/2]+1}^{[s/2]} y_{i+j}^O, \quad (13)$$

$$i = [(s+1)/2], [(s+1)/2] + 1, \dots, N - [s/2].$$

Herein, the size of the moving window is identical with  $s$  in  $\hat{S}_{DE}(s)$ . The consequent de-trended series  $y^D$

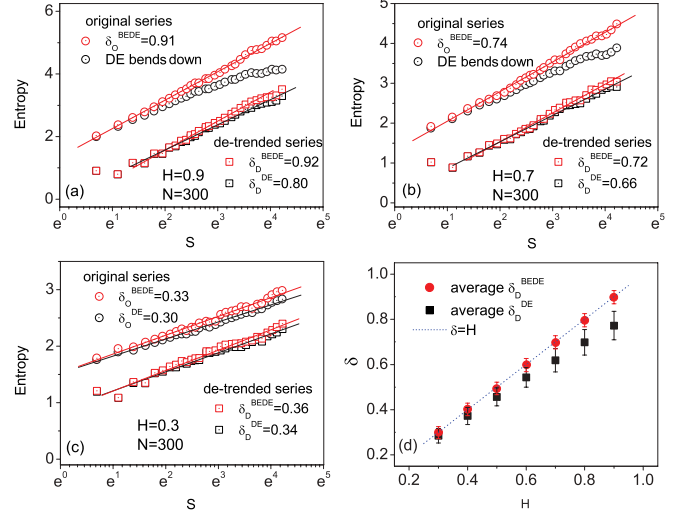


FIG. 1. (Color online) Performance of the centered moving average. The series are fractional Brownian motions with length 300. (a)–(c) Results for three series with  $H = 0.9, 0.7$ , and  $0.3$ , respectively. The BEDE method can accurately estimate  $\delta$  from the original and detrended series. The DE curve for the original series bends down. The DE can detect scale invariance in the detrended series. Confidence intervals for the estimated values are all less than 0.02. (d) Bias and deviation of the DE and BEDE estimations for the detrended series. The BEDE can estimate the scaling exponent without bias and with higher precision, while the DE underestimates the scaling exponent by up to 10% with lower precision.

reads

$$y_i^D = y_i^O - y_i^T, \quad (14)$$

$$i = [(s+1)/2], [(s+1)/2] + 1, \dots, N - [s/2].$$

Fractional Brownian motions are generated to investigate the performance of the centered moving average. Figures 1(a)–1(c) present results for three series with Hurst exponents  $H = 0.9, 0.7$ , and  $0.3$ , as typical examples. The DE and BEDE methods are used to estimate  $\delta$  values for the original signals and the corresponding detrended series. The curves show that from the detrended series the BEDE method can obtain almost the same values of  $\delta$  as those from the original series, namely, in the BEDE method the centered moving average does not introduce artificial characteristics. From the original series, the BEDE method can obtain correctly the values of  $\delta$ , while the DE method cannot find scaling invariance in signals with larger values of  $H$  (the curves bend down, especially for signals with large  $H$ ). Figure 1(d) shows the variance and bias (mean) of the exponents for the detrended series estimated by using the DE and BEDE, respectively. The average is taken over 1000 series with length 300 for each  $H$ . One can see that the BEDE method can estimate  $\delta$  for signals with  $0 < \delta < 1$  without bias and with higher precision, while the DE method underestimates  $\delta$  by up to 10% and has lower precision.

## III. RESULTS

### A. Scaling behaviors for sleep stages

Figure 2(a) shows the heartbeat interval series for subject number 59 as part of a typical record. One can see that

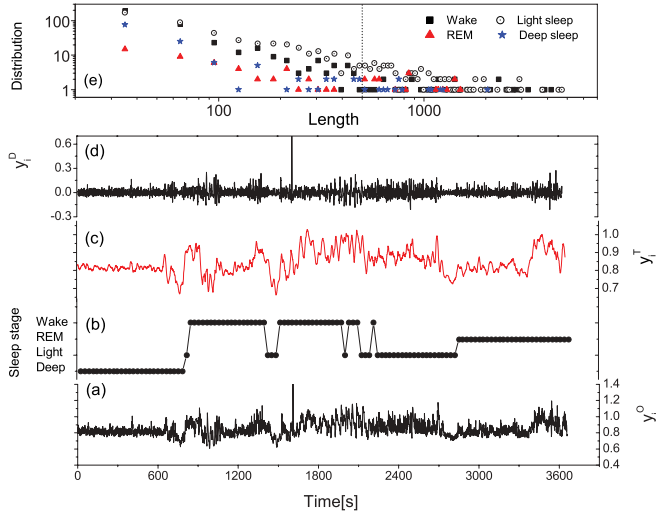


FIG. 2. (Color online) EEG records. (a) Part of the heartbeat interval series for subject 59 shown as an example. (b) Sleep stages annotated by visual evaluation of electrophysiological recordings of brain activity. (c) Trend extracted from the original series in (a). The trend for  $s = 21$  is shown as an example. (d) Detrended series for  $s = 21$  as an example. (e) Lengths for waking, light sleep, REM sleep, and deep sleep stages distributed in the interval  $10^1-10^3$  (without characteristic lengths).

transitions between different sleep stages occur frequently, as annotated in Fig. 2(c). There exists a complicated and significant trend [see Fig. 2(c), in which the trend for  $s = 21$  is shown as an example]. The corresponding detrended series is depicted in Fig. 2(d). From all the records one can see that most of the durations for the waking, light sleep, REM sleep, and deep sleep stages are distributed in the interval  $10^1-10^3$  (without characteristic lengths), as presented in Fig. 2(e).

As a typical example, we show in Figs. 3(a)–3(d) results for the segments 7290–8520 s (waking), 8520–9270 s (light sleep), 9270–10 110 s (REM sleep), and 6450–7290 s (deep

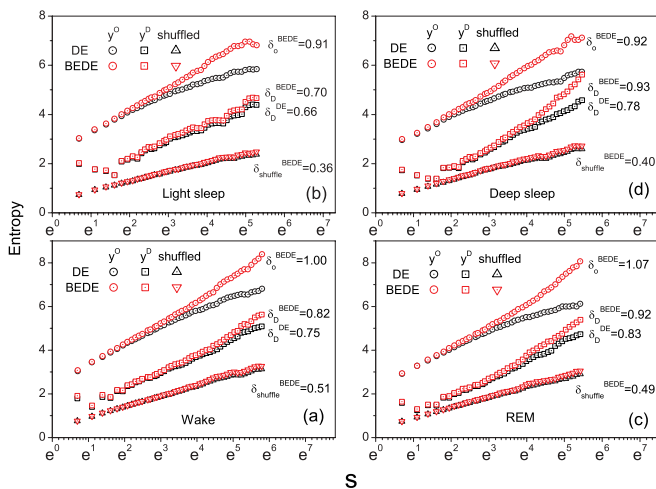


FIG. 3. (Color online) Scaling behaviors in a sleep cycle of subject 59. (a)–(d) Scaling behaviors of the segments 7290–8520 s (waking), 8520–9270 s (light sleep), 9270–10 110 s (REM sleep), and 6450–7290 s (deep sleep), respectively. Confidence intervals for estimated values are all less than 0.02.

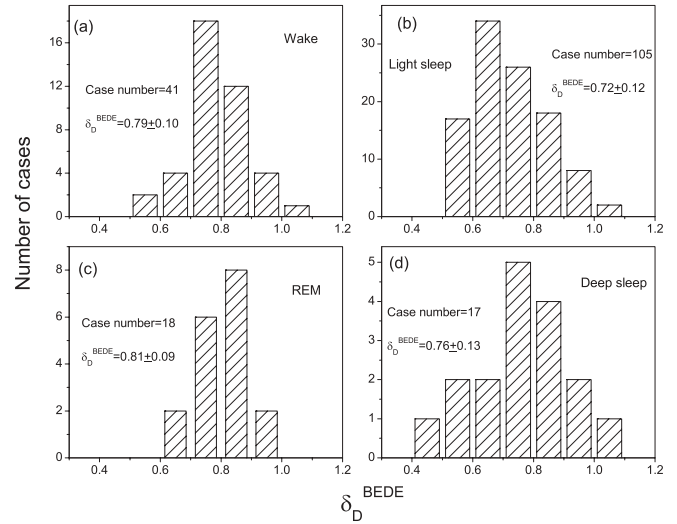


FIG. 4. Distribution of scaling exponents for different sleep stages. From all the subjects the segments corresponding to waking, light sleep, REM sleep, and deep sleep are extracted. Segments whose lengths are less than 500 are discarded. (a)–(d) Scaling exponent distributions for waking, light sleep, REM sleep, and deep sleep. The average values for REM sleep and waking are significantly larger ( $\sim 0.8$ ) those for light sleep ( $\sim 0.7$ ).

sleep), which forms a sleep cycle of subject 59. One can see that the curves for the DE results bend down with the increase of scale, while this trend is corrected by use of the BEDE method to straight lines in a considerable range of scale. What is more, although the BEDE can detect successfully scaling behaviors in the original series, the estimated values of the scaling exponents are significantly larger than those for the corresponding detrended series. From the original series the estimations for waking, light sleep,

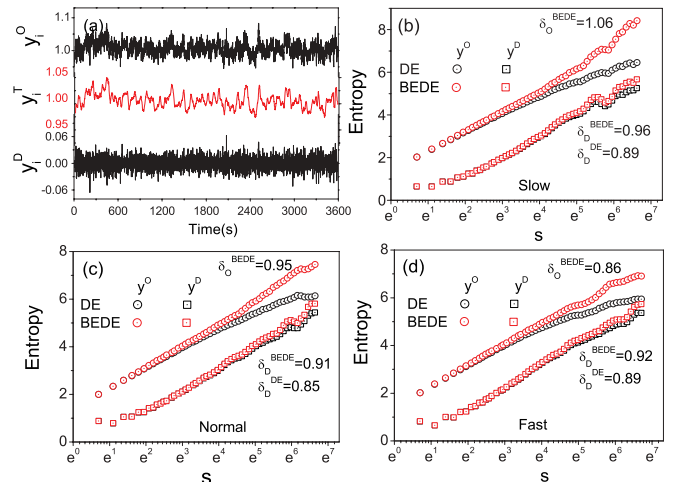


FIG. 5. (Color online) Scale invariance of stride series. (a) Stride interval series from normal walk record of the volunteer si01, and the corresponding trend and detrended series. The trend and detrended series for  $s = 21$  are shown as an example. (b)–(d) Scaling behaviors in slow, normal, and fast walk series. For the detrended series, the values estimated by using the DE are very close to (generally smaller than) those obtained by using the BEDE. Confidence intervals for the estimated values are all less than 0.02.



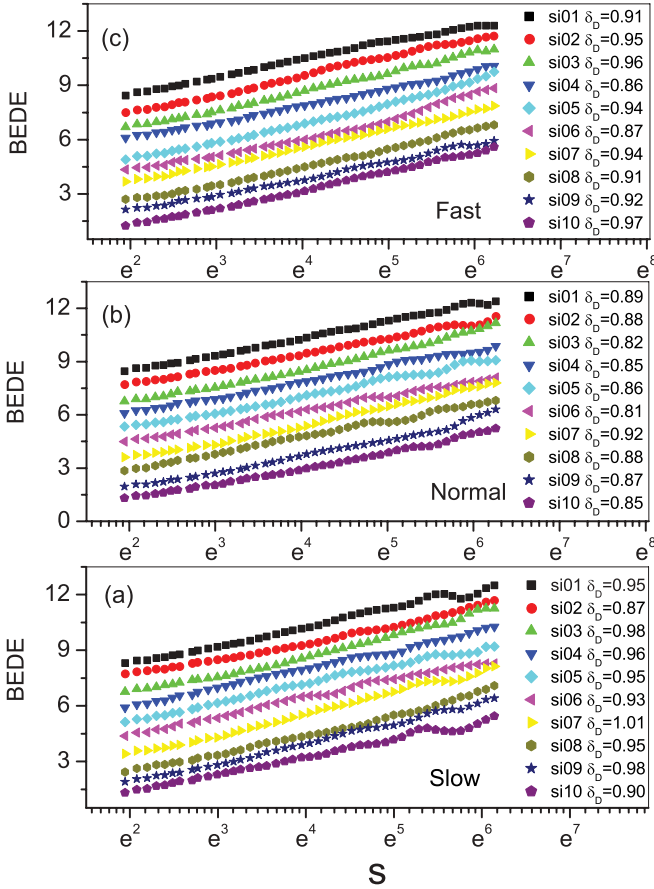


FIG. 6. (Color online) The BEDE results of detrended series for all ten volunteers. (a)–(c) Scaling behaviors embedded in slow, normal, and fast series (detrended). Confidence intervals for the estimated values are all less than 0.02.

REM sleep, and deep sleep are 1.00, 0.91, 1.07, and 0.92, while those from the corresponding de-trended series are 0.82, 0.70, 0.92, and 0.93. For the detrended series, the DE underestimates the exponents by up to 10%. Hence, to obtain reliable scaling behaviors for the different sleep stages we must conduct a detrending procedure and use the BEDE instead of the DE. Results for shuffled detrended series tell us that the scaling behaviors come from nontrivial patterns in the series rather than distribution of the elements in the series.

From all the subjects we extract the segments corresponding to waking, light sleep, REM sleep, and deep sleep, whose lengths are larger than 500 (about a duration of 450 s), the numbers of which are 41, 105, 18, and 17, respectively. The distribution behaviors of the values for scaling exponent are presented in Figs. 4(a)–4(c). One can see that the average value and standard deviation of the scaling exponent for REM sleep are almost the same as those for waking, but the distribution for the former is much more sharply peaked than that for the latter. The average value and standard deviation for light sleep are almost identical with those for deep sleep, while the detailed shapes for the distributions are completely different. Obviously, to confirm whether the differences in distributions originate from intrinsic behaviors or just from statistical errors requires collection of a large number of cases.

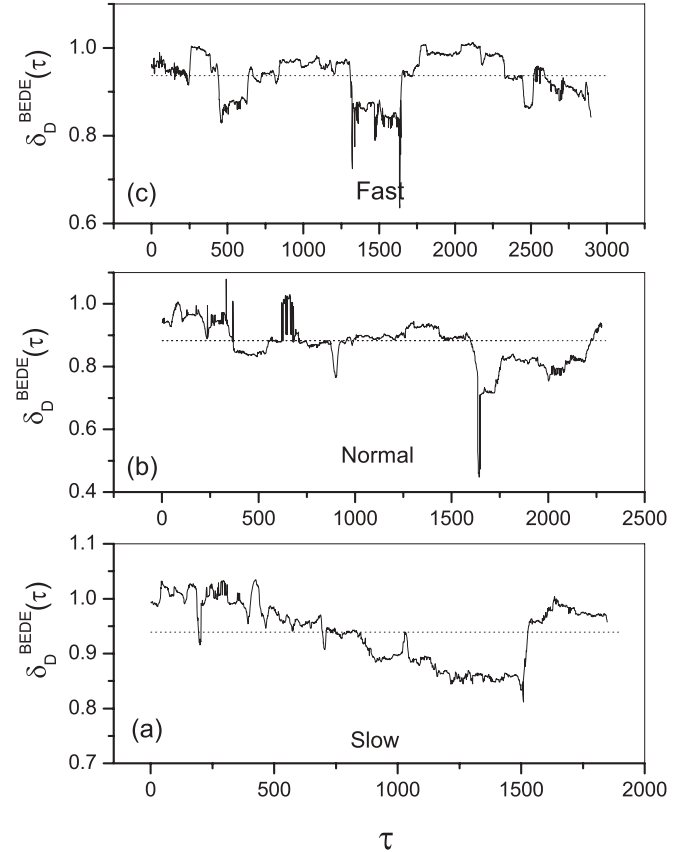


FIG. 7. Evolution of scaling behaviors in the stride records. (a)–(c) Scaling behaviors embedded in slow, normal, and fast walk records of the volunteer si01. The scaling exponents oscillate abruptly over wide ranges.  $\Delta\tau = 700$ .

What is more, the average values for REM sleep and waking are significantly larger ( $\sim 0.8$ ) than those for light sleep ( $\sim 0.7$ ).

### B. Scaling behaviors for stride series

From the stride records, one can calculate the corresponding stride interval series, trends, and detrended series. As an example, see in Fig. 5(a) the results from the normal walking record of the volunteer si01. For slow, normal, and fast walks the lengths of the series are 3304, 3371, and 3395, respectively, which are significantly larger than those of the sleep stages. For the original series, with an increase of scale the DE curves bend down, i.e., scaling behavior cannot be detected successfully, while the BEDE curves are almost perfect straight lines over considerably wide scales, as shown in Figs. 5(b)–5(d). However, the estimated values of the scaling exponents from the original series may be unacceptably large compared with those from the corresponding detrended series (e.g., the difference for the slow record is 0.10). Consequently, the detrending procedure is the key step to obtaining reliable estimations of the scaling exponent. What is more, the values estimated by using the DE are very close to (generally smaller than) those obtained by using the BEDE, and this conclusion stands for all the ten volunteers (not presented).

The BEDE results for the detrended series  $y^D$  for all ten volunteers are shown in Fig. 6. The BEDE curves are almost perfect straight lines over a considerable width of scale; the

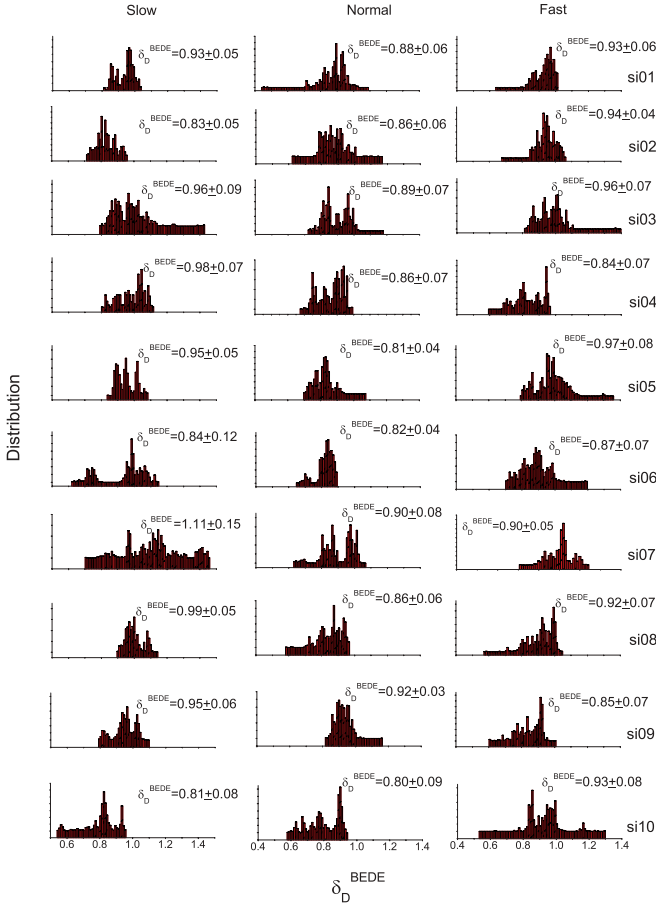


FIG. 8. (Color online) Distribution details of the evolutionary scaling exponents for slow, normal, and fast walking series of all ten volunteers. Details of the distributions are completely different from each other.  $\Delta\tau = 700$ .

estimations of the scaling exponents, namely, the slopes of the curves, are also presented.

An interesting question is whether the physiological states of the volunteers remain unchanged in the walking experiments. Sliding a window along a detrended series, at the  $\tau$ th step the window covers segment  $y_\tau^D, y_{\tau+1}^D, \dots, y_{\tau+\Delta\tau-1}^D$ , where  $\Delta\tau$  is the size of the window. Representing the local scaling behavior at step  $\tau$  by the scaling exponent for the segment covered by the window, denoted by  $\delta_D^{\text{BEDE}}(\tau)$ , the successive values of  $\delta_D^{\text{BEDE}}(\tau)$ ,  $\tau = 1, 2, \dots, N - \Delta\tau + 1$ , present the evolution of the scaling behavior of the considered series. As a typical result, Figs. 7(a)–7(c) provide the evolutions of the scaling behaviors embedded in the slow, normal, and fast walk records of volunteer si01. Figure 8 provides the distribution details and the mean and standard values of the evolutionary scaling exponents for slow, normal, and fast walking series of all the volunteers. Unexpectedly, the scaling exponents oscillate abruptly over wide ranges and the details of the local scaling exponent distributions are completely different from each other.  $\Delta\tau$  is chosen to be 700 in the calculations.

#### IV. CONCLUSIONS

Scale invariance in physiological signal records attracts special attention for its importance in understanding and

consequent modeling of physiological phenomena and its potential usage in diagnoses and therapy. But evaluation of the scale invariance in physiological signals is a nontrivial task. Theoretically, variance-based methods may lead to a failure in evaluation of the scaling behavior. In practice, a physiological signal generally is itself very short ( $\sim 10^2$ ), or separated by frequent occurrences of phase transitions into short segments. In the literature, persistent efforts have been made to find reliable methods to evaluate scale invariance in short time series [22].

In the present paper, we extract waking, light sleep, REM sleep, and deep sleep segments (length greater than 500 for reliable estimation of scaling exponents) from long-term EEG signals. By means of the concept of balanced estimation of diffusion entropy, we estimate the scaling exponents of detrended series constructed from the segments. It is found that for each stage the scaling value is distributed over a considerably wide range, i.e., the scaling behavior is subject and sleep cycle dependent. Statistically, the average of the scaling exponent values for waking segments is almost the same as that for REM sleep segments ( $\sim 0.8$ ), while the average of the scaling exponent values for light sleep segments is  $\sim 0.7$ .

For the stride series, because the series are long enough (3000–4000), the original diffusion entropy and balanced estimation of diffusion entropy give almost the same results for detrended series. But from the evolutions of the local scaling invariance one can see that the physiological states change abruptly, although in the experiments great efforts were made to keep conditions unchanged. Hence, the global behavior of a single physiological signal may lose rich information about physiological states.

In comparing the results from the DE and BEDE methods, one can see that the BEDE can evaluate with considerable precision scale invariance in very short time series ( $\sim 10^2$ ). The original DE method sometimes underestimates the value of the scaling exponent, or even cannot detect the scaling behavior due to the bias of bending down as the scale increases. The two methods (BEDE and DE) are both sensitive to trends in time series. In the BEDE concept, the existence of a trend may lead to an unreasonably high value of the scaling exponent, which may lead to mistaken conclusions. Hence, the balanced estimation of diffusion entropy is a preferential candidate for correct and precise evaluation of scale invariance in short time series, provided that the time series is detrended properly.

#### ACKNOWLEDGMENTS

The work is supported by the National Science Foundation of China under Grants No. 10975099 and No. 50974052, the Program for Professors of Special Appointment (Eastern Scholar) at Shanghai Institutions of Higher Learning, the Innovation Program of Shanghai Municipal Education Commission under Grant No. 13YZ072, and the Shanghai leading discipline project under Grant No. S30501. One of the authors (W.Z.) acknowledges the support of the Innovation Fund Project For Graduate Students of Shanghai under Grant No. JWCXSL1102. We thank the reviewers for their stimulating and constructive comments and suggestions.

- [1] M. Small, *Applied Nonlinear Time Series Analysis: Applications in Physics, Physiology and Finance*, Nonlinear Science Series A, Vol. 52 (World Scientific, Singapore, 2005).
- [2] B. J. West, *Front. Phys.* **1**, 12 (2010).
- [3] M. Kobayashi and T. Musha, *IEEE Trans. Biomed. Eng.* **29**, 456 (1982); C.-K. Peng, J. Mietus, J. M. Hausdorff, S. Havlin, H. E. Stanley, and A. L. Goldberger, *Phys. Rev. Lett.* **70**, 1343 (1993); C.-K. Peng, S. Havlin, H. E. Stanley, and A. Li. Goldberger, *Chaos* **5**, 82 (1995).
- [4] P. Ch. Ivanov, A. Bunde, L. A. N. Amaral, S. Havlin, J. Fritschyelle, R. M. Baevsky, H. E. Stanley, and A. L. Goldberger, *Europhys. Lett.* **48**, 594 (1999); A. Bunde, S. Havlin, J. W. Kantelhardt, T. Penzel, J.-H. Peter, and K. Voigt, *Phys. Rev. Lett.* **85**, 3736 (2000); J. W. Kantelhardt, Y. Ashkenazy, P. Ch. Ivanov, A. Bunde, S. Havlin, T. Penzel, J.-H. Peter, and H. E. Stanley, *Phys. Rev. E* **65**, 051908 (2002); C.-C. Lo, L. A. Nunes Amaral, S. Havlin, P. Ch. Ivanov, T. Penzel, J.-H. Peter, and H. E. Stanley, *Europhys. Lett.* **57**, 625 (2002).
- [5] P. Ch. Ivanov, L. A. N. Amaral, A. L. Goldberger, S. Havlin, M. G. Rosenblum, Z. R. Struzik, and H. E. Stanley, *Nature (London)* **399**, 461 (1999); J. W. Kantelhardt, E. Koscielny-Bunde, D. Rybski, P. Braun, A. Bunde, and S. Havlin, *J. Geophys. Res.* **111**, D01106 (2005).
- [6] C.-K. Peng, S. V. Buldyrev, S. Havlin, M. Simons, H. E. Stanley, and A. L. Goldberger, *Phys. Rev. E* **49**, 1685 (1994); K. Hu, P. Ch. Ivanov, Z. Chen, P. Carpena, and H. E. Stanley, *ibid.* **64**, 011114 (2001); H. E. Stanley, J. W. Kantelhardt, S. A. Zschiegner, E. Koscielny-Bunde, S. Havlin, and A. Bunde, *Physica A* **316**, 87 (2002); B. Podobnik and H. E. Stanley, *Phys. Rev. Lett.* **100**, 084102 (2008); B. Podobnik, D. Horvatic, A. M. Petersen, and H. E. Stanley, *Proc. Natl. Acad. Sci. USA* **106**, 22079 (2009).
- [7] N. Scafetta, P. Hamilton, and P. Grigolini, *Fractals* **9**, 193 (2001); P. Grigolini, L. Palatella, and G. Raffaelli, *ibid.* **9**, 439 (2001); N. Scafetta and P. Grigolini, *Phys. Rev. E* **66**, 036130 (2002).
- [8] N. Scafetta, *Fractal and Diffusion Entropy Analysis of Time Series: Theory, Concepts, Applications and Computer Codes for Studying Fractal Noises and Levy Walk Signals* (VDM Verlag Dr. Muller, Saarbrücken, Germany, 2010).
- [9] M. S. Roulston, *Physica D* **125**, 285 (1999).
- [10] J. A. Bonachela, H. Hinrichsen, and M. A. Muñoz, *J. Phys. A* **41**, 202001 (2008).
- [11] J. Qi and H. Yang, *Phys. Rev. E* **84**, 066114 (2011).
- [12] P. Grigolini, D. Leddon, and N. Scafetta, *Phys. Rev. E* **65**, 046203 (2002); N. Scafetta and B. J. West, *Phys. Rev. Lett.* **90**, 248701 (2003); N. Scafetta, P. Grigolini, T. Imholt, J. Roberts, and B. J. West, *Phys. Rev. E* **69**, 026303 (2004); N. Scafetta, and B. J. West, *Phys. Today* **61** (3), 50 (2008); *Phys. Rev. Lett.* **105**, 219801 (2010).
- [13] H. Yang, F. Zhao, L. Qi, and B. Hu, *Phys. Rev. E* **69**, 066104 (2004).
- [14] H. Yang, F. Zhao, W. Zhang, and Z. Li, *Physica A* **347**, 704 (2005); S. Cai, P. Zhou, H. Yang, C. Yang, B. Wang, and T. Zhou, *ibid.* **367**, 337 (2006); N. Scafetta, R. Moon, and B. J. West, *Complexity* **12**, 12 (2007); S. Cai, P. Zhou, H. Yang, T. Zhou, B. Wang, and F. Zhao, *Physica A* **375**, 687 (2007); N. Scafetta, D. Marchi, and B. J. West, *Chaos* **19**, 026108 (2009).
- [15] C. Acquisti, P. Allegrini, P. Bogani, M. Buiatti, E. Catanese, L. Fronzoni, P. Grigolini, G. Mersi, and L. Palatella, *Chaos Solitons Fractals* **20**, 127 (2004); F. Zhao, H. Yang, and B. Wang, *J. Theor. Biol.* **247**, 645 (2007).
- [16] N. Scafetta and B. J. West, *Phys. Rev. Lett.* **92**, 138501 (2004); *Complexity* **10**, 51 (2005); C.-Y. Tsai and C.-F. Shieh, *Physica A* **387**, 5561 (2008).
- [17] S. Cai, P. Zhou, H. Yang, C. Yang, B. Wang, and T. Zhou, *Physica A* **367**, 337 (2006); J. Perello, M. Montero, L. Palatella, I. Simonsen, and J. Masoliver, *J. Stat. Mech.: Theor. Exp.* (2006) P11011.
- [18] See <http://www.physionet.org/physiobank/database/slpdb/>.
- [19] See <http://physionet.org/physiobank/database/umwdb/>.
- [20] P. Allegrini, V. Benci, P. Grigolini, P. Hamilton, M. Ignaccolo, G. Menconi, L. Palatella, G. Raffaelli, Nicola Scafetta, M. Virgilio, and J. Yang, *Chaos Solitons Fractals* **15**, 517 (2003); M. Rypdal and K. Rypdal, *Phys. Rev. Lett.* **104**, 128501 (2010); **105**, 219802 (2010).
- [21] E. Alessio, A. Carbone, G. Castelli, and V. Frappietro, *Eur. Phys. J. B* **27**, 197 (2002); A. Carbone, G. Castelli, and H. E. Stanley, *Phys. Rev. E* **69**, 026105 (2004); L. Xu, P. Ch. Ivanov, K. Hu, Z. Chen, A. Carbone, and H. E. Stanley, *ibid.* **71**, 051101 (2005); D. Grech and Z. Mazur, *Acta Phys. Pol. B* **36**, 2403 (2005); A. Bashan, R. Bartsch, J. W. Kantelhardt, and S. Havlin, *Physica A* **387**, 5080 (2008); Z.-Q. Jiang and W.-X. Zhou, *Phys. Rev. E* **84**, 016106 (2011).
- [22] R. Oliver and J. L. Ballester, *Phys. Rev. E* **58**, 5650 (1998); S. Katsev and I. L'Heureux, *Comput. Geosci.* **29**, 1085 (2003); M. G. Ogurtsov, *Sol. Phys.* **220**, 93 (2004); D. Delignieres, S. Ramdani, L. Lemoine, K. Torre, M. Fortes, and G. Ninot, *J. Math. Psychol.* **50**, 525 (2006); M. Scheffer, J. Bascompte, W. A. Brock, V. Brovkin, S. R. Carpenter, V. Dakos, H. Held, E. H. Van Nes, M. Rietkerk, and G. Sugihara, *Nature (London)* **461**, 55 (2009); S. R. Carpenter, J. J. Cole, M. L. Pace, R. Batt, W. A. Brock, T. Cline, J. Coloso, J. R. Hodgson, J. F. Kitchell, D. A. Seekell, L. Smith, and B. Weidel, *Science* **332**, 1079 (2011).